IBRO Reports 6 (2019) 31–39

Contents lists available at ScienceDirect

IBRO Reports

journal homepage: www.elsevier.com/locate/ibror

Research Paper

Acoustic white noise ameliorates reduced regional brain expression of CaMKII and ΔFosB in the spontaneously hypertensive rat model of ADHD

Daniel Eckernäs*, Fredrik Hieronymus, Thomas Carlsson, Filip Bergquist

Department of Pharmacology, Inst of Neuroscience and Physiology, Sahlgrenska Academy at University of Gothenburg, Sweden

ARTICLE INFO

Keywords:
Attention deficit hyperactivity disorder
Immunohistochemistry
Image analysis
CaMKII
ΔFosB
Acoustic white noise

ABSTRACT

Loud (≥70dBA) acoustic white noise improves cognitive performance in children with ADHD as well as skilled reach and rotarod performance in the spontaneously hypertensive (SH) rat model of ADHD. To investigate how acoustic noise influences the brain activity in the SH rat model of ADHD, immunohistochemical staining of two neuronal activity and plasticity markers, Ca^{2+}/Calmodulin dependent protein kinase II (CaMKII) and ΔFosB, was evaluated in Wistar (n = 24) and SH (n = 16) rats after repeated exposure to acoustic noise or ambient silence. Other SH rats (n = 6) were treated with repeated methylphenidate (MPH). Expression of CaMKII was reduced in the tuberomammillary nucleus (TMN) of the SH rat compared to Wistar but not in the nucleus accumbens (nAc) or the dorsolateral prefrontal cortex (DL-PFC). In the TMN, the expression of CaMKII was increased by noise in both strains. ΔFosB expression was reduced in nAc, DL-PFC and the dorsolateral striatum (DLS) of the SH rat compared to Wistar. Exposure to acoustic white noise significantly increased ΔFosB expression in the nAc and DL-PFC but not in the DLS of SH rats. The results indicate that acoustic noise shifts a reduced neuronal activity in the nAc, TMN and DL-PFC in SH rats toward the normal levels of activity in outbred rats. This may explain why noise has benefit selectively in ADHD.

1. Introduction

ADHD is a neurodevelopmental disorder with a prevalence of 5–7% amongst children in the developed world (Thomas et al., 2015). The disorder is associated with considerable negative individual outcomes relating to educational attainment (Hinshaw, 1992; Fergusson and Horwood, 1995; Barry et al., 2002), anti-social behavior (Satterfield et al., 1994; McKay and Halperin, 2001) and co-morbidity (Steinhausen et al., 2006). The main symptoms of the disorder include hyperactivity, inattention and impulsivity (American Psychiatric Association, 2013).

Although efficacious behavioral therapies are available (Knouse et al., 2017), pharmacological treatment remains central in the management of moderate to severe ADHD. Dopaminergic stimulants like amphetamine and methylphenidate (MPH) can ameliorate both hyperactivity and cognitive symptoms in children, adolescents and adults (Spencer et al., 1996; Barbaresi et al., 2006; Santosh et al., 2011; Bilder et al., 2016). However, stimulant treatment is associated with adverse effects like poor appetite, insomnia, stomachaches and headaches (Barkley et al., 1990), and have a risk for abuse (Clemow and Walker, 2014). Furthermore, long-term use of stimulants has been linked to growth suppression (Spencer et al., 1996; Swanson et al., 2017). Despite the positive effects of stimulant treatments on cognitive performances in ADHD it is not evident that they enhance learning processes (Molina et al., 2009). The adverse effects and other limitations of stimulants make them less useful for people with mild symptoms or significant co-morbidity (Shier et al., 2013). Therefore, new or improved pharmacological and non-pharmacological interventions are needed.

A recently proposed non-pharmacological intervention for ADHD is loud (≥70 dBA) acoustic white noise. The idea is derived from a study demonstrating unexpected beneficial effects of acoustic noise for cognitive performance in children with ADHD (Söderlund et al., 2007). Improved cognitive performance during noise exposure appears to be specific for children with low baseline attention, because in normally developed children noise has negative effects (Söderlund et al., 2007,

Abbreviations: CaMKII, Ca2 + /calmodulin-dependent protein kinase II; DL-PFC, dorsolateral prefrontal cortex; DLS, dorsolateral striatum; FosB, finkel-biskis-jinkins murine osteosarcoma viral oncogene homolog B; MD, mean difference; MPH, methylphenidate; nAc, nucleus accumbens; SH, spontaneously hypertensive rat; SHM, spontaneously hypertensive rat methylphenidate treatment; SHN, spontaneously hypertensive rat noise condition; SHS, spontaneously hypertensive rat silence condition; TMN, tuberomammillary nucleus; WIN, wistar noise condition; WIS, wistar silence condition

* Corresponding author at: University of Gothenburg, Institute of Neuroscience and Physiology, Department of Pharmacology, Box 431, 405 30, Gothenburg, Sweden.

E-mail address: Daniel.eckernas@neuro.gu.se (D. Eckernäs).

https://doi.org/10.1016/j.ibror.2018.11.007
Received 1 August 2018; Accepted 28 November 2018

2010). Replicating studies have interestingly demonstrated that acoustic noise benefit seems to be independent of stimulant ADHD medication (Allen and Pammer, 2015; Söderlund et al., 2016). A beneficial effect of acoustic noise has also been found in the spontaneously hypertensive (SH) rat model of ADHD where loud white noise improves rotarod performance and the learning of skilled reach in SH rats, but not in a Wistar control strain (Söderlund et al., 2015).

The mechanism of acoustic noise benefit in ADHD and the ADHD rat model is not known, but could at least theoretically involve an increase in cortical arousal, the masking of irrelevant stimuli (Durlach et al., 2003) or some form of stochastic resonance phenomenon in the CNS (Moss et al., 2004; Sikström and Söderlund, 2007).

The SH rat displays core ADHD like symptoms at a young age (up to 12 weeks), and is presently the best validated animal model of the disorder (Sagvolden, 2000). Micro-array studies have revealed that, in the SH rat, the expression of the plasticity marker Ca^{2+} /Calmodulin dependent protein kinase II (CaMKII) is significantly decreased in the medial prefrontal cortex, ventral striatum, dorsal striatum, hippocampus, vermis, and ventral mesencephalon (DasBanerjee et al., 2008). Furthermore, the expression of CaMKII and components of the Fos family of immediate early genes have been reported to be decreased in the nucleus accumbens of SH rats (Papa et al., 1996, 1997, 1998), a decrease that may be reversed by MPH (Sadile, 2000)

CaMKII is a highly abundant Ca^{2+} activated kinase in the mammalian brain. It is prominently expressed in the postsynaptic density (Erondu and Kennedy, 1985), and has an important role for the induction of long term potentiation (Lisman et al., 2012). Altered activity of CaMKII has been implicated in the SH model and can be normalized by methylphenidate (Yabuki et al., 2014).

The transcription factor FosB and its truncated splice variant ΔFosB are immediate early genes which are upregulated a few hours after increased cellular activity. ΔFosB accumulates following repeated exposures to an activating stimulus like addictive drugs, stress or natural rewards (Nestler et al., 2001; Perrotti et al., 2004).

In order to identify the possible mechanisms of action of acoustic noise benefit in the ADHD phenotype we have in this study investigated the expression of CaMKII and ΔFosB in the brains of SH and Wistar rats following repeated exposure of loud acoustic noise, and in SH rats in response to MPH.

2. Experimental procedures

2.1. Animals

A total of 22 male spontaneously hypertensive rats (SHR/NCrl, Charles River, Germany), 16 male Wistar (Crl:WI(Han), Charles River, Germany) and 8 male Wistar (RccHan:WIST, Harlan Laboratories, United Kingdom) were used in the study. The animals were four weeks of age and weighed between 100–140 g at the beginning of the study. They were housed in cages of four under 12 h light/dark cycles with *ad libitum* access to food and water. All animal handling and experiments were conducted in accordance with Swedish animal welfare legislation and the European Union directive 2010/63/EU on the protection of animals used for scientific purposes. An ethical approval (No. 101/16) of the experimental design was acquired from the Gothenburg Animal Research Ethics Committee.

2.2. Experimental groups

Animals were stratified to the following treatment groups: Wistar kept in ambient silence (WIS, n = 12), SH kept in ambient silence (SHS, n = 8), Wistar exposed to acoustic noise (WIN, n = 12), SH exposed to acoustic noise (SHN, n = 8) and SH treated with MPH (SHM, n = 6). Animals from different vendors were equally distributed between groups.

2.3. Treatment

Animals were placed together with their home cage littermates in a transparent plastic transport cage (35 × 35 x 25 cm) and exposed to either 75 dBA acoustic white noise, ambient silence for one hour per day or, in the case of MPH, one hour of ambient silence after receiving an intraperitoneal injection with 4 mg/kg MPH, for a total of 5 consecutive days. During the treatment period the cages were covered with a piece of dark cloth to reduce visual stimuli.

2.4. Perfusion and fixation procedure

Forty-eight hours after the final treatment the animals were sacrificed for immunohistochemical analysis of the brain. Deep anesthesia was induced with sodium pentobarbital (120 mg/kg) and the animal was then perfused trans-cardially with 20–50 ml physiological saline (≈ 1 min, until runoff liquid was clear) immediately followed by 200 ml freshly made ice-cold 4% paraformaldehyde solution in 0.1 M phosphate buffer, pH 7.4, for 7 min. The brain was removed and post-fixed in 4% paraformaldehyde in 0.1 M phosphate buffer, pH 7.4, overnight in 4 °C before being transferred to a 25% sucrose solution. All brains were sectioned into 35 μm thick slices using a cryostat (Leica CM1950, Leica Biosystems, Heidelberg, Germany), divided in to 8 series and stored in a cryo-protectant solution at −20 °C until staining.

2.5. Immunostaining protocol

Free-floating sections were first washed 3 x 10 min in PBS. Heat induced epitope retrieval was performed by submerging the sections in heated sodium citrate buffer (10 nM) containing 0.05% Tween-20, pH 6.0, and placed in a 90 °C water bath for 6 min. Further, to block endogenous peroxidase activity free floating sections were quenched in PBS containing 3% H_2O_2 and 10% methanol during gentle agitation. Sections were thereafter first pre-incubated in 5% normal horse or goat serum (Vector laboratories, Burlingame, CA) containing 0.25% Triton-X in PBS, followed by overnight incubation with well-established and specific primary antibodies against either CaMKIIα (mouse, 1: 2000; ab22609; 6G9; Abcam, Cambridge, UK; Jarome et al., 2013; Zhong et al., 2014; Tada et al., 2016; Leroy et al., 2017; Roy et al., 2017) or ΔFosB (Rabbit, 1:5000; SC-48X; Santa Cruz Biotechnology, Dallas, Tx; Djakovic et al., 2012; Sanz-Blasco et al., 2018). On the second day sections were incubated using an appropriate biotinylated secondary antibody (1:250 horse anti mouse BA2001 for CaMKIIα and 1:250 goat anti rabbit BA1000 for ΔFosB; Vector Laboratories,) for one hour followed by one hour incubation in avidin-biotin peroxidase in PBS (ABC Elite Kit, Vector Laboratories). Finally, the staining was visualized by the chromogen 3, 3´-diaminobenzidine (DAB) in PBS containing H_2O_2 (DAB Peroxidase substrate kit, Vector Laboratories). Sections were left in DAB for 5 min or until satisfactory background staining was achieved, the staining process was then stopped with an excess of PBS and the sections were then washed 3 x 10 min in PBS. To achieve satisfactory results, the CaMKIIα staining had to be re-stained over 5 min in DAB directly following the washing step. Sections were mounted on poly-L-lysine coated glass slides (Histobond, Marienfeld, Lauda-Königshofen, Germany), dried over 72 h, washed in dH_2O, dehydrated in ascending ethanol solution, cleared in xylene and cover-slipped with DPX mounting medium for microscopy (Merck Millipore, Darmstadt, Germany).

2.6. Evaluation of activated brain areas

All analysis of stained sections was performed on slides that had been coded to blind the assessor to strain and treatment conditions. To allow an unbiased evaluation of possible differences in CaMKII expression, sections from throughout the brain from the prefrontal cortex to the brainstem (at the level of locus coeruleus) were first visually

Table 1
Brain areas visually inspected during CaMKII whole-brain screening (n = 16). Images were visually compared between blind coded groups and if a difference was suspected the area was quantified by image analysis and evaluated statistically. Three regions (Dorsolateral prefrontal cortex, Nucleus Accumbens and Tuberomammilary nucleus) showed significant treatment and/or strain difference and was together with the dorsolateral striatum included in the full sample and analysis.

Region	Visually suspected difference after image comparison.	p-value			Included in the second batch
		Treatment	Strain	Interaction	
Dorsolateral prefrontal cortex	Yes	.20	.86	**.022**	Yes
Nucleus Accumbens (core and shell)	Yes	.82	.38	**.027**	Yes
Tuberomammilary nucleus	Yes	**.006**	**.003**	.42	Yes
Dorsolateral Striatum	N/A	–	–	–	Yes
Locus coeruleus	Yes	.29	.08	.16	No
Subthalamic nucleus	Yes	.47	.61	.67	No
Dorsal raphe nucleus	Yes	.07	.49	.099	No
Pedunculopontine nucleus	No	–	–	–	No
Entopenduncular nucleus	No	–	–	–	No
Substantia Nigra	No	–	–	–	No
Orbital cortex	No	–	–	–	No
Thalamic nucleus (various parts)	No	–	–	–	No
Hippocampus	No	–	–	–	No
Cingulate cortex	No	–	–	–	No

evaluated in a subset consisting of 16 animals (WIS, n = 4, WIN, n = 4, SHS, n = 4, SHN, n = 4). The purpose was to identify brain areas with visually suspected differences in CaMKII expression in between the groups. Throughout the screening process when a brain structure which prominently expressed CaMKII was encountered, the area was photographed and images from the four different treatment groups were visually compared to detect any indication of differences between the groups (Table 1). Altogether approximately 3200 stained sections were visually assessed for CaMKII expression in this way. In brain areas where differences in CaMKII expression between animals was suspected, as well as in areas previously established as important for the ADHD phenotype, the number of CaMKII positive cell bodies or CaMKII staining intensity were quantified by computerized image analysis. The outcome was statistically analyzed (see Statistics) and for the areas where significant differences could be observed (Table 1), the image analysis was repeated on the full material. The same areas were also analyzed regarding ΔFosB. Data acquired from all animals were used in the final statistical analysis. “The rat brain in stereotaxic coordinates, 6th ed” (Paxinos and Watson, 2009) was used to determine the location of investigated brain areas.

2.7. Image acquisition and workflow for quantification of staining

Image acquisition was performed using a light microscope (Nikon Eclipse 90i; Nikon Instruments inc., Shinagawa, Tokyo, Japan) and images were captured using a CCD camera (Nikon DS-Fi1-U2; Nikon Instruments inc., Shinagawa, Tokyo, Japan). The microscope imaging software used was NIS Elements D (V 4.40; Nikon Instruments inc., Shinagawa, Tokyo, Japan). Images were analyzed using Fiji version 1.51 s for Windows (Schindelin et al., 2012).

A standardized work flow for cell counting was established in the Fiji software. Removal of irrelevant background noise was performed by applying 50 iterations of Gaussian blur (sigma = 3) to the original image (*Img1 A*; Fig. 1A). A new image (*Img1B*; Fig. 1B) was created from *Img1 A* and its blurred counterpart using the algorithm (*Img1B = min (Img1 A, Img1 A blurred*). Subtraction of the background was performed by applying 100 iterations of Gaussian blur (sigma = 4) to *Img1B* and a new image (*Img1C*; Fig. 1C) was created by using the subtraction algorithm (*Img1C = Img1B – Img1B blurred*). *Img1C* was converted to 8-bit color depth and a local threshold value was determined by the Phansalkar algorithm (radius = 15, Parameter_1 = 0.19, Parameter_2 = 0.9; Fig. 1D; (Neerad et al., 2011)). To separate cells that appeared joined together after thresholding, a watershed operation was performed. The region of interest was selected and cells was counted using “Analyze Particles” (size = 40–200; circularity 0.5–1.0; Fig. 1E).

To compensate for different background intensities of the ΔFosB staining, threshold values in each individual image were established by sampling the mean grayscale intensity of ΔFosB activated cells. Background noise was removed by applying the algorithm (*Img1B = min(Img1 A, Img1 A blurred*) and five visually identified ΔFosB activated cells was selected and the mean grayscale pixel value were measured. A threshold value was set to cover all pixels ranging from zero to ten grayscale units brighter than the mean pixel value measured for the activated ΔFosB cells. This was to assure that pixels at the edges of each active cell, which tend to be brighter, were included in the analysis. After thresholding the image was converted to binary, a watershed operation was performed and cells were counted using “Analyze Particles” (size = 30–300; circularity 0.5–1.0).

Mean neuronal staining intensity calculations in the tuberomammillary nucleus (TMN) were also performed using Fiji software. The unprocessed image was converted to 8-bit, and the colors were inverted to negative. The background intensity was determined by selecting three regions bordering to, but not including, TMN. The mean intensity of these selections was used as a reference point for background staining. The difference between TMN intensity and background staining was used in the statistical analysis.

All sections analyzed in the whole-brain subsample were re-blinded and re-analyzed together with the full sample and un-blinding was done after all image analysis had been completed.

The ImageJ scripts used for these procedures and the dataset collected can be supplied on request.

2.8. Statistics

Cell counts and grayscale intensities were analyzed using linear mixed models. Measurements from different brain areas were analyzed independently and separate analyses were run for CaMKII and ΔFosB, respectively. Due to the lack of a proper control group for MPH-treated animals (SHM), the primary analysis only included data from noise and silent-treated animals.

The mixed model used for the primary analysis of both the whole-brain subsample and the full sample included fixed factors for strain (Wistar or SH) and treatment (silence or noise), as well as the interaction between strain and treatment. If the interaction term was non-significant ($p > .05$) it was omitted and the model was rerun with only the two fixed effects included. Post-hoc tests are reported if either the treatment by strain interaction, or one of the main effects from the reduced models, were significant ($p \leq .05$). To accurately reflect the

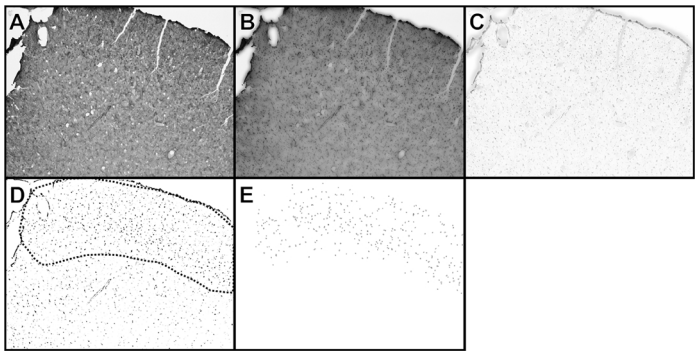

Fig. 1. Image analysis work-flow. The acquired photographed original image (A; Img1 A), was processed using noise removal by application of a minimum algorithm to Img1 A and its blurred counterpart (B; Img1B). Following removal of background staining using a subtract algorithm on Img1B and its blurred counterpart (C; Img1C), a Local threshold determined by Phansalkar algorithm was applied to Img1C (D). Region of interest was finally outlined (black dotted line; D) and particles were analyzed, giving the counted cells within the region of interest (E).

raw data, estimated means and post-hoc tests are reported for the interaction model. Post hoc p-values are reported without correction for multiple testing. Post hoc comparisons between SHS and WIN were not deemed relevant and are therefore not reported even if significant ($p \leq .05$).

Separate linear mixed models were used to assess the effects of MPH-treatment as compared to the noise and silent condition. As MPH-treatment was administered to SH-rats only, Wistar rats were excluded from these analyses. The model included a three-level fixed factor indicating the received treatment (silence, noise or MPH). If the overall test of treatment effects was significant ($p < .05$), we report post-hoc tests for the comparisons between SHM and SHN, and SHM and SHS, respectively.

For all models, within-subject correlations between measurements from left and right hemispheres were modelled using a compound symmetry (co)variance matrix and the Kenward-Roger approximation was used to estimate denominator degrees of freedom. All analyses were conducted in SAS software version 9.4 (SAS Institute, Cary, NC, USA).

3. Results

Results from the whole-brain subsample are summarized in Table 1. The areas that showed significant effects of noise on CaMKII staining in the whole-brain subsample were nucleus accumbens (nAc), dorsolateral prefrontal cortex (DL-PFC) and TMN. These areas were then re-analyzed in the full sample for both CaMKII and ΔFosB expression. In the Dorsolateral striatum (DLS) we saw no quantifiable staining of CaMKII. However, since the striatum is strongly connected to the DL-PFC we chose to include it in the analysis of ΔFosB staining. Because there was no quantifiable ΔFosB staining in the TMN, this area was not included in the ΔFosB analysis.

3.1. Nucleus accumbens

Although there was a significant interaction between noise treatment and strain for CaMKII positive cells in the nAc in the whole brain analysis (Table 1), no difference regarding CaMKII expression in the nAc were found in the analysis of the full data set as indicated by a non-significant interaction ($F(1, 36) = 1.67$, $p = 0.21$) or main effects of strain ($F(1, 37) = 1.76$, $p = 0.19$) or noise ($F(1, 37) = 1.37$, $p = 0.25$; Fig. 2A).

In contrast, there were clear differences in the numbers of ΔFosB positive cells in the nAc between the different treatment conditions. Analysis of the full sample revealed a significant strain × noise interaction ($F(1, 36) = 7.42$, $p = 0.01$; Fig. 2B) but no main effects of strain ($F(1, 36) = 0.02$, $p = 0.89$) or noise ($F(1, 36) = 0.92$, $p = 0.34$). Post hoc tests indicated that the interaction was explained by lower ΔFosB expression in the nAc in SH rats than in Wistar rats exposed to the ambient silence condition (MD: -76.0 cells; $p = 0.050$) and that noise-treatment (MD: 97.6 cells; $p = 0.023$) increased the activity in the nAc in SH rats, but had no significant effect in the nAc of Wistar animals (MD: -46.8 cells; $p = 0.17$).

3.2. Dorsolateral prefrontal cortex

In the analysis of CaMKII expression in the DL-PFC (Fig. 3A) there were no significant strain × noise interaction ($F(1, 36) = 2.59$, $p = 0.12$), main effects of strain ($F(1, 37) = 0.60$, $p = 0.44$) or noise ($F(1, 37) = 1.52$, $p = 0.23$).

In the analysis of ΔFosB positive cells in the DL-PFC (Fig. 3B) there was a main effect of strain ($F(1, 37) = 4.21$, $p = 0.047$) and of treatment ($F(1, 37) = 4.47$, $p = 0.041$) but no interaction ($F(1, 36) = 3.54$, $p = 0.068$). Post hoc tests indicated that in the ambient silence condition SH rats had significantly fewer ΔFosB positive cells in the DL-PFC than Wistar animals (MD: -64.9; $p = 0.0075$). Noise treatment was associated with higher counts of ΔFosB positive cells in the DL-PFC in SH rats (MD: 71.3; $p = 0.0074$), but not in Wistar rats (MD: 10.3; $p = 0.62$).

3.3. Tuberomammillary nucleus

There were no ΔFosB positive cells in the TMN. However, a difference in CaMKII fiber expression between conditions was observed (Fig. 4). The analysis revealed significant main effects of strain ($F(1, 36.8) = 14.52$, $p < 0.001$) and of noise ($F(1, 37.4) = 6.18$, $p = 0.018$) but no interaction ($F(1, 35.7) = 0.06$, $p = 0.81$). SH rats exposed to the ambient silence condition, had significantly less CaMKII expression than Wistar rats (MD: -11.2; $p = 0.0087$). According to the post hoc tests, noise did not increase the expression of CaMKII in the SH (MD: 7.5; $p = 0.091$) or Wistar rats (MD: 6.2; $p = 0.088$) compared to their ambient silence controls. However, in contrast to SH rats kept in ambient silence, SH rats exposed to the noise condition did not display significantly less CaMKII expression than Wistar rats exposed to the ambient silence condition (MD: -3.7; $p = 0.34$).

3.4. Dorsolateral striatum

No CaMKII positive cells were found in the DLS in the different conditions (Fig. 5). The analysis of ΔFosB positive cells revealed a main effect of strain ($F(1, 37) = 13.62$, $p < 0.001$) but not of noise ($F(1, 37) = 0.69$, $p = 0.41$) and no interaction ($F(1, 36) = 0.49$, $p = 0.49$). The strain effect was evident between SH and Wistar animals exposed to the ambient silence control condition, where SH animals had fewer ΔFosB positive cells (MD: -70.6; $p = 0.0039$) as well as in animals exposed to white acoustic noise where the ΔFosB positive cells were also fewer in SH animals than in Wistar (MD: -47.9; $p = 0.043$). Noise did not increase ΔFosB expression in the SH rat (MD: 26.7; $p = 0.29$).

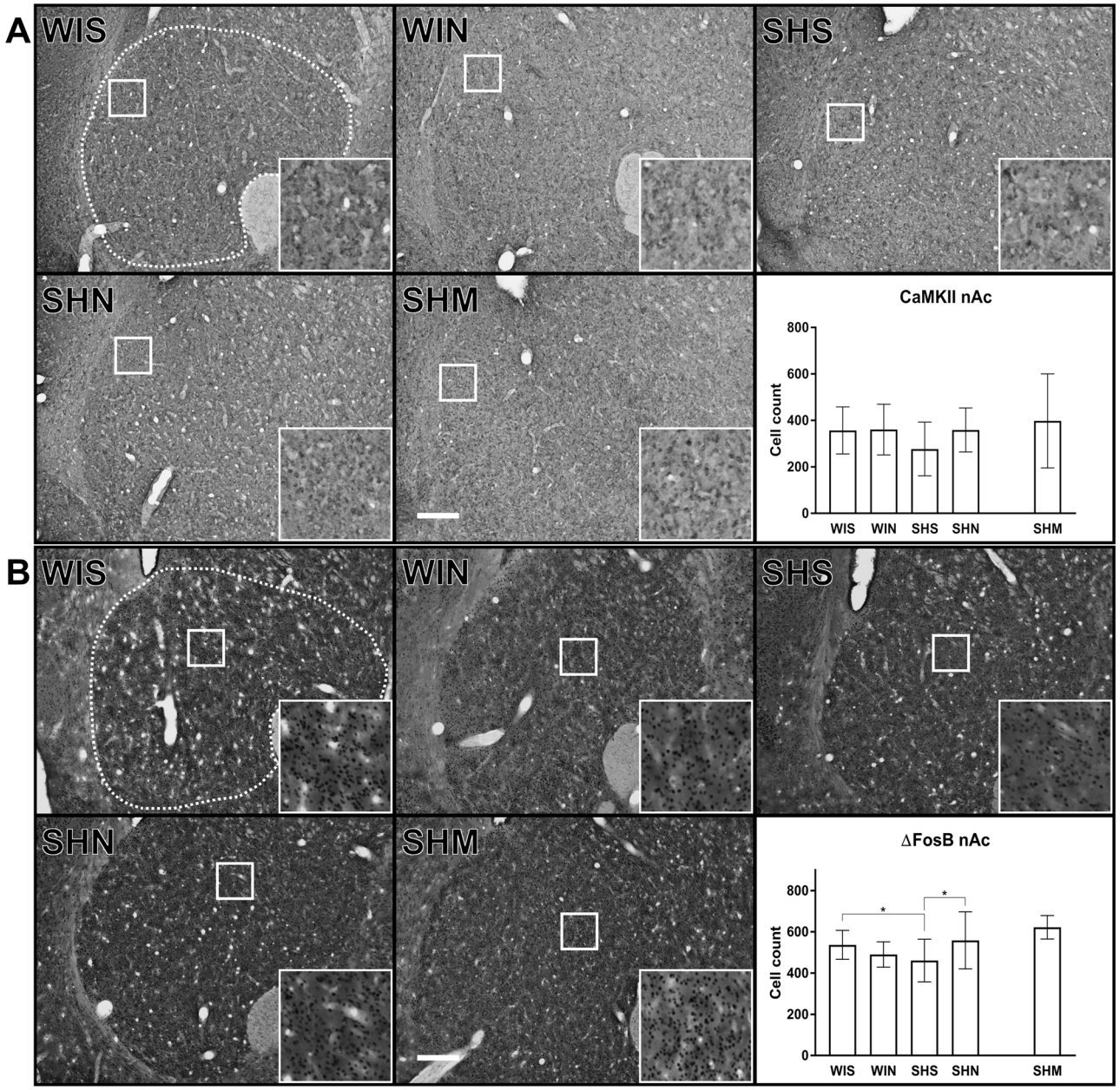

Fig. 2. CaMKII (A) and ΔFosB (B) positive cell count in nucleus accumbens (nAc). We found no significant differences in CaMKII expression in the nAc (A). ΔFosB cell counts showed a significant reduction in nAc in SH rats as compared to Wistar, this reduction was reversed following noise (B; SHS vs WIS (p = 0.050); vs SHN (p = 0.023). The white dotted line indicated in the WIS images represents the regions of analysis for the corresponding area. The inserts represent a 9x magnification of the area indicated by the solid white square. The contrast has been slightly enhanced equally in all inserts for viewing purposes. The white scale bar in the SHM images represent 250 μm. Wistar-silence (WIS), Wistar-noise (WIN), SH-silence (SHS, SH-noise (SHN), SH-methylphenidate (SHM). (*) indicate significant between group post-hoc tests. Cell count values represent Mean ± SD. Processed images of the analysis of CaMKII and ΔFosB can be found as supplementary Fig. 1.

3.5. Effects of methylphenidate as compared to the noise and silent conditions in SH-rats

Similar to the effects of noise, MPH treatment did not significantly alter CaMKII-expression in the DL-PFC ($F(2, 19) = 2.03$, $p = .16$) or nAc ($F(2, 19) = 1.77$, $p = .20$). When looking only at SH rats, there was no effect of treatment on CaMKII-expression in TMN ($F(2, 18.3) = 2.42$, $p = .12$). Conversely, MPH treatment did significantly increase ΔFosB expression in the DL-PFC as compared to the silent (MD 86.8, $p = .005$) but not the noise condition (MD 15.5, $p = .58$) (omnibus $F(2, 19) = 6.24$, $p = .008$). Similarly, ΔFosB expression in the nAc was significantly increased by MPH treatment as compared to the silent (MD 161.2, $p = .008$) but not the noise condition (MD 63.5, $p = .26$) (omnibus $F(2, 19) = 4.64$, $p = .023$). With regards to the DLS, MPH increased ΔFosB expression both compared to the silent (MD 93.8, $p = .002$) and the noise condition (MD 67.1, $p = .02$) (omnibus $F(2, 19) = 6.61$, $p = .007$).

4. Discussion

The overall result of this study is that the expression of the neuronal activity/plasticity markers ΔFosB and CaMKII tends to be lower in several brain areas in the SH rat model of ADHD and that this difference can be reduced by acoustic noise in a fashion that resembles, but is not identical to the effects of MPH. Consequently it appears that repeated acoustic noise can normalize plasticity markers in some brain areas

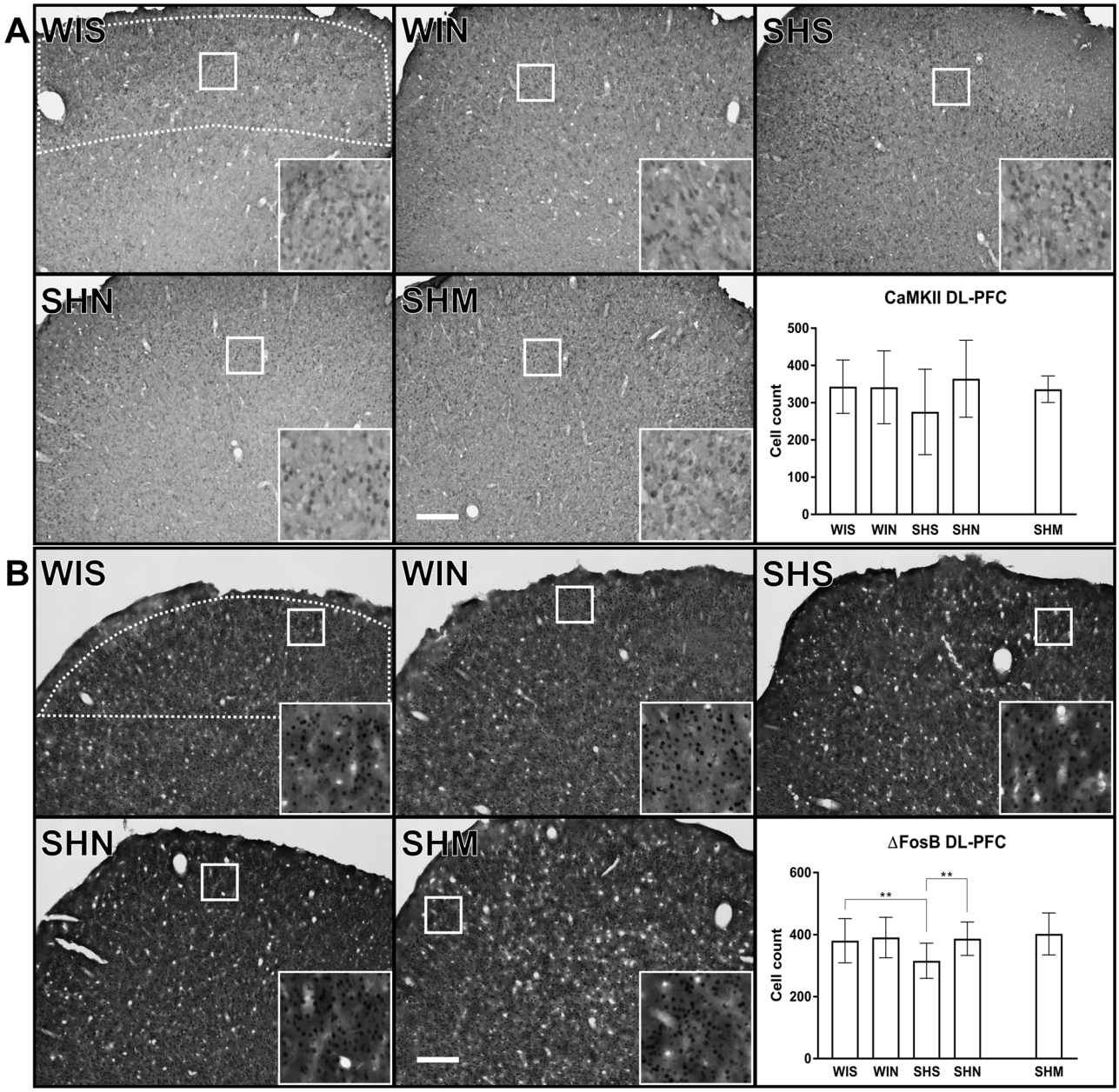

Fig. 3. CaMKII (A) and ΔFosB (B) positive cell count in the dorsolateral prefrontal cortex (DL-PFC). We found no significant differences in CaMKII expression in the DL-PFC (A). ΔFosB in DL-PFC was significantly altered in SH rats compared to Wistar rats (B). This effect was rescued following noise treatment (B; SHS vs WIS ($p = 0.0075$); vs SHN ($p = 0.0074$). The white dotted line indicated in the WIS images represents the regions of analysis for the corresponding area. The inserts represent a 9x magnification of the area indicated by the solid white square. The contrast has been slightly enhanced equally in all inserts for viewing purposes. The white scale bar in the SHM images represent 250 μm. Wistar-silence (WIS), Wistar-noise (WIN), SH-silence (SHS), SH-noise (SHN), SH-methylphenidate (SHM). (*) indicate significant between group post-hoc tests. Cell count values represent Mean ± SD. Processed images of the analysis of CaMKII and ΔFosB can be found as supplementary Fig. 2.

known to influence cognition and behavior in the SH rat ADHD model (Russell, 2000, 2002, 2003).

The DL-PFC receives, among other, sensory inputs from the auditory sensory system and is important for top-down control of motor behaviors (Miller and Cohen, 2001). Reduced activation of the DL-PFC is congruent with the ADHD phenotype of the SH rat, as well as with known alterations of brain activity and structure in children and adolescents with ADHD (Dickstein et al., 2006; Cao et al., 2013; Dimatelis et al., 2015). It is therefore intriguing that this study shows that both MPH and acoustic noise can ameliorate the reduction in DL-PFC ΔFosB activity in SH rats as it suggests similar effect pathways of the two interventions. Furthermore, the effect of acoustic noise is strain specific, or conditioned by a reduced baseline expression of ΔFosB. A significant interaction strain × noise was found for CaMKII expression in the subpopulation analysis. However, in the full population there was a larger variability in CaMKII-expression and no significant effects of strain or noise could be confirmed. It is a limitation of this study that it is likely underpowered for detecting changes in CaMKII-expression.

Like the DL-PFC, the NAc responds to reward feedback and forms part of the corticostriatal reward system important for habit learning. The anatomical connections between the prefrontal cortex and the ventral striatum implies that the observed similarity of ΔFosB activity patterns between the DL-PFC and the NAc may be the result of functional interactivity. However, the NAc is more strongly connected to the

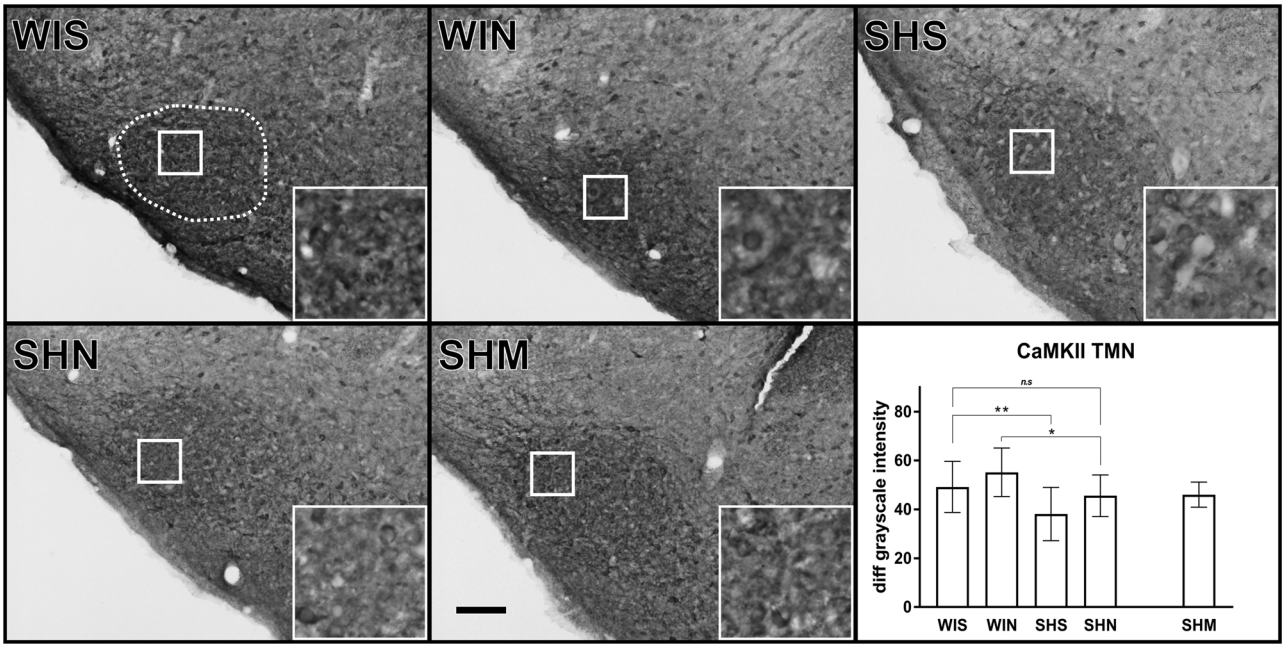

Fig. 4. CaMKII staining intensity in the tuberomammillary nucleus (TMN). Cells were not stained in the TMN, but a general increase of staining intensity was observed in this region. A significantly decreased staining was observed in SH rats as compared to Wistar rats SHS vs WIS ($p = 0.0087$). CaMKII expression in both strains were increased following acoustic white noise exposure indicated by a main effect of noise ($p = 0.019$). Values are reported as difference between neuronal intensity and background staining. The white dotted line indicated in the WIS image represents the region of analysis. The inserts represent a 9x magnification of the area indicated by the solid white square. The contrast has been slightly enhanced equally in all inserts for viewing purposes. The black scale bar in the SHM image represents 100 µm. Wistar-silence (WIS), Wistar-noise (WIN, SH-silence (SHS, SH-noise (SHN), SH-methylphenidate (SHM). (*) indicate significant between group post-hoc tests. Grayscale intensity values represent Mean ± SD.

medial parts of the prefrontal cortex than the lateral parts that display changed ΔFosB activity in this study. In the context of acoustic noise it is interesting that tinnitus is associated mainly with increased activity in the NAc (Leaver et al., 2011). Acute administration of MPH increases dopamine and noradrenaline levels in both the prefrontal cortex and the striatum of SH rats, as reviewed in Heal et al. (2008), but chronic administration may have more specific catecholamine-enhancing effects in the prefrontal cortex than in the NAc (Koda et al., 2010).

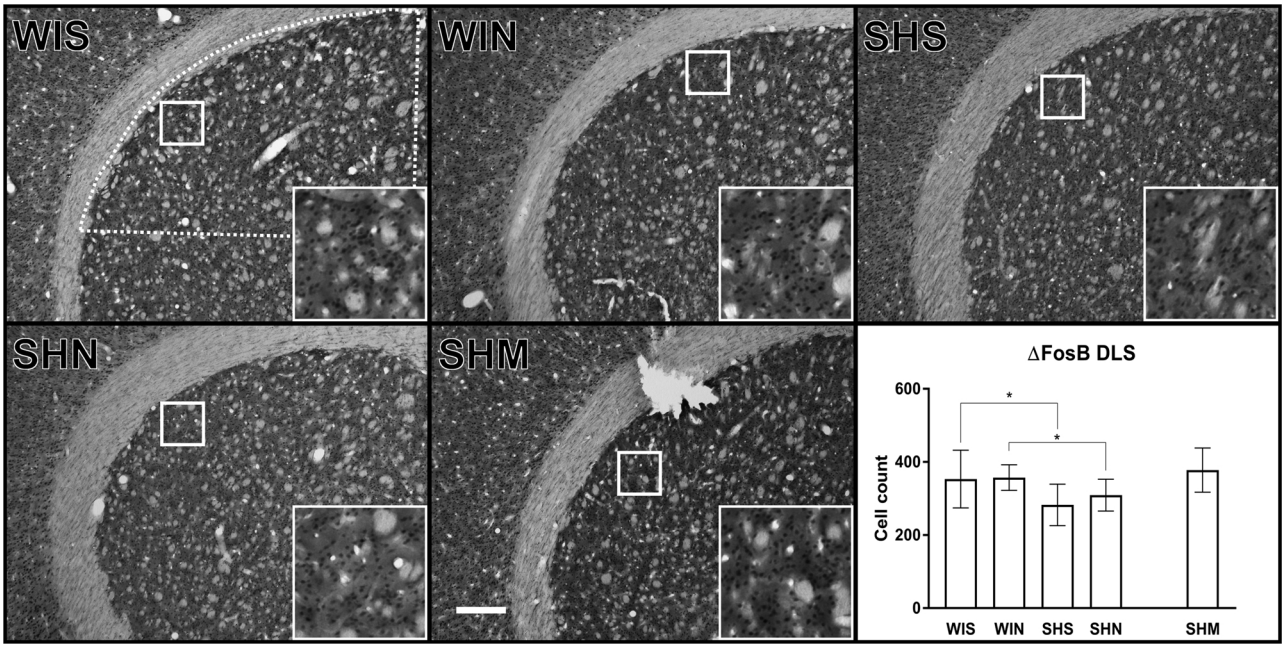

Fig. 5. ΔFosB positive cells in the dorsolateral striatum (DLS). A significantly decreased number of cells was observed in SH rats as compared to Wistar rats SHS vs WIS ($p = 0.0039$). This change was not affected by noise, SHS vs SHN ($p = 0.29$). The white dotted line indicated in the WIS image represents the region of analysis. The inserts represent a 9x magnification of the area indicated by the solid white square. The contrast has been slightly enhanced equally in all inserts for viewing purposes. The white scale bar in the SHM image represents 250 µm. Wistar-silence (WIS), Wistar-noise (WIN, SH-silence (SHS), SH-noise (SHN), SH-methylphenidate (SHM). (*) indicate significant between group post-hoc tests. Cell count values represent Mean ± SD. Processed images of the analysis of CaMKII can be found as supplementary Fig. 3.

Although we find similar changes in ΔFosB positive cells in the DL-PFC and NAc after MPH and acoustic noise, this is an observational result that does not necessarily indicate that it is the change in activity that mediates the observed effects of MPH and noise on cognitive functions and skilled motor learning. If this was the case one could predict that persons with ADHD may find symptom relief in tinnitus, but to our knowledge there are no observations supporting this notion.

In previous studies, reduced expression of CaMKII was found regionally in the nAc of the SH rat (Papa et al., 1996, 1998). The nAc was not sampled by subdivisions in this study and therefore we cannot confirm these earlier findings.

It is important to notice that unlike many other studies we chose to not use the inbred Wistar Kyoto strain as control. The rational for that has been discussed previously (Söderlund et al., 2015), but in short, the reason for not doing so is to avoid exaggerated genetic effects by using genetically more variable strains. It is possible that the difference between SH rats and outbred Wistar rats is less pronounced than between SH rats and the Wistar Kyoto strain and this may warrant further investigation.

The DL-PFC is more strongly connected to the DLS than to the nAc (Averbeck et al., 2014; Haber, 2016). It can therefore be expected to find a correlation between effects of strain and treatment in the DLS and the DL-PFC. In the DLS, however, acoustic noise did not increase ΔFosB positive cells in SH rats as it did in the DL-PFC. An increase in ΔFosB positive cells in the DLS was nevertheless found following MPH treatment. This suggests that MPH treatment compared to acoustic nose activates the DLS to a larger proportion than the DL-PFC. A possible explanation for this is that the origin of the effect of acoustic noise on the DL-PFC is external and comes from sources that project more to the PFC than the DLS, whereas MPH exerts its effects directly in areas with dense dopamine and noradrenaline terminals. Notably, CaMKII was not expressed in the DLS following either treatment in the two rat strains.

In the TMN where the histamine cell bodies that regulate arousal and wakefulness are located (Haas and Panula, 2003), there was no ΔFosB expression, suggesting that the cellular activity was not responsive to the treatment conditions, however, there were clear differences in the CaMKII expression, again with lower levels in SH rats. Noise treatment increased the levels of CaMKII in both strains. The difference in CaMKII expressing fibers between the two strains may represent a difference in the activity of afferents to histaminergic cell bodies or other neuronal structures in the TMN. The afferent pathways to the TMN mainly consist of projections from the infralimbic cortex (ventromedial prefrontal cortex), hypothalamus and the basal forebrain, and to a lesser extent from the brain stem (Ericson et al., 1991). As there is a considerable convergence of afferents from many parts of the brain we can only speculate to the significance of the observed difference in CaMKII positive fibers in the TMN of SH rats. It is nevertheless possible that it represents altered regulation of histaminergic neurons in SH rats.

The cortical arousal hypothesis (or the optimum stimulation theory) as proposed by Zentall and Zentall (1983) states that individuals with ADHD suffer from a state of suboptimal cortical arousal as a result of aberrant neurotransmission or inadequate central stimulation. According to this theory people with ADHD compensate a lack of arousal by hyperactivity or increased verbalization. Stimulant medication is recognized to increase cortical arousal and alertness (see Wood et al., 2014 for a review) and its efficacy in reducing ADHD symptoms fits well into Zentall & Zentalls theory of low arousal. In the TMN, the synthesis of histamine has been shown to be mediated through CaMKII phosphorylation (Torrent et al., 2005). The increased CaMKII expression observed in both strains following acoustic white noise exposure could therefore be interpreted in terms of altered arousal through increased histamine production. On the contrary, both the fact that white noise applications are popular sleeping aids and observations regarding the role of acoustic noise for arousal and sleep (Stanchina et al., 2005; Messineo et al., 2017) suggest that acoustic white noise will increase the threshold needed to elicit an arousal event, possibly by masking other acoustic stimuli. Since our data does not allow us to measure histamine expression, further research is needed to determine what outcome increased CaMKII expression in the TMN would have on histamine synthesis and cortical arousal.

Important limitations of the current study include that no whole brain analysis of ΔFosB was performed before focusing the analysis to a restricted subset of areas. The ΔFosB analysis is therefore not exhaustive. FosB/ ΔFosB is not uniquely expressed in neurons (Nomaru et al., 2014) and other cell populations may contribute to the change in signal. Further, only male rats were included in the study which may influence the generalizability of the results. The CaMKII antibody used is selective for the α-subunit which is almost exclusively found in excitatory neurons (Liu and Jones, 1996, 1997) and does not bind to the β-subunit expressed in glia cells (Ouimet et al., 1984). However, the results in the present study demonstrate the relative change in total CaMKII and does not distinguish between phosphorylated and non-phosphorylated CaMKII expression which may be an issue of further investigation.

In summary, the results suggest that acoustic white noise appears to induce changes in brain activity in some brain areas (DL-PFC, TMN and nAc), but not in DLS. The effect of acoustic white noise in the prefrontal cortex in particular suggests that it could help to normalize top-down control of behavior, but presumably via other mechanisms than MPH. The genetic activation patterns observed after noise exposure in the SH rat model of ADHD strengthen the notion that acoustic white noise may be a useful non-pharmacological strategy for treating ADHD.

Funding

This research did not receive any specific grant from funding agencies in the public, commercial, or not-for-profit sectors.

Conflict of interest

The Authors declare they have no conflict of interests.

References

Allen, R., Pammer, K., 2015. The impact of concurrent noise on visual search in children with ADHD. J. Atten. Disord.

American Psychiatric Association, 2013. Diagnostic and Statistical Manual of Mental Disorders: DSM-5.

Averbeck, B.B., Lehman, J., Jacobson, M., Haber, S.N., 2014. Estimates of projection overlap and zones of convergence within frontal-striatal circuits. J. Neurosci. 34, 9497–9505.

Barbaresi, W.J., Katusic, S.K., Colligan, R.C., Weaver, A.L., Leibson, C.L., Jacobsen, S.J., 2006. Long-term stimulant medication treatment of attention-deficit/hyperactivity disorder: results from a population-based study. J. Dev. Behav. Pediatr. 27, 1–10.

Barkley, R.A., McMurray, M.B., Edelbrock, C.S., Robbins, K., 1990. Side effects of methylphenidate in children with attention deficit hyperactivity disorder: a systemic, placebo-controlled evaluation. Pediatrics 86, 184.

Barry, T.D., Lyman, R.D., Klinger, L.G., 2002. Academic underachievement and attention-deficit/Hyperactivity disorder. J. Sch. Psychol. 40, 259–283.

Bilder, R.M., Loo, S.K., McGough, J.J., Whelan, F., Hellemann, G., Sugar, C., Del'Homme, M., Sturm, A., Cowen, J., Hanada, G., McCracken, J.T., 2016. Cognitive effects of stimulant, Guanfacine, and combined treatment in child and adolescent Attention-Deficit/Hyperactivity disorder. J. Am. Acad. Child Adolesc. Psychiatry 55, 667–673.

Cao, Q., Shu, N., An, L., Wang, P., Sun, L., Xia, M.R., Wang, J.H., Gong, G.L., Zang, Y.F., Wang, Y.F., He, Y., 2013. Probabilistic diffusion tractography and graph theory analysis reveal abnormal white matter structural connectivity networks in drug-naive boys with attention deficit/hyperactivity disorder. J. Neurosci. 33, 10676–10687.

Clemow, D.B., Walker, D.J., 2014. The potential for misuse and abuse of medications in ADHD: a review. Postgrad. Med. 126, 64–81.

DasBanerjee, T., Middleton, F.A., Berger, D.F., Lombardo, J.P., Sagvolden, T., Faraone, S.V., 2008. A comparison of molecular alterations in environmental and genetic rat models of ADHD: a pilot study. Am. J. Med. Genet. B Neuropsychiatr. Genet. 147B, 1554–1563.

Dickstein, S.G., Bannon, K., Castellanos, F.X., Milham, M.P., 2006. The neural correlates of attention deficit hyperactivity disorder: an ALE meta-analysis. J. Child Psychol. Psychiatry 47, 1051–1062.

Dimatelis, J.J., Hsieh, J.H., Sterley, T.L., Marais, L., Womersley, J.S., Vlok, M., Russell, V.A., 2015. Impaired energy metabolism and disturbed dopamine and glutamate signalling in the striatum and prefrontal cortex of the spontaneously hypertensive rat

model of attention-deficit hyperactivity disorder. J. Mol. Neurosci. 56, 696–707.
Djakovic, S.N., Marquez-Lona, E.M., Jakawich, S.K., Wright, R., Chu, C., Sutton, M.A., Patrick, G.N., 2012. Phosphorylation of Rpt6 regulates synaptic strength in hippocampal neurons. J. Neurosci. 32, 5126–5131.
Durlach, N.I., Mason, C.R., Shinn-Cunningham, B.G., Arbogast, T.L., Colburn, H.S., Kidd Jr., G., 2003. Informational masking: counteracting the effects of stimulus uncertainty by decreasing target-masker similarity. J. Acoust. Soc. Am. 114, 368–379.
Ericson, H., Blomqvist, A., Kohler, C., 1991. Origin of neuronal inputs to the region of the tuberomammillary nucleus of the rat brain. J. Comp. Neurol. 311, 45–64.
Erondu, N.E., Kennedy, M.B., 1985. Regional distribution of type II Ca2+/calmodulin-dependent protein kinase in rat brain. J. Neurosci. 5, 3270–3277.
Fergusson, D.M., Horwood, L.J., 1995. Early disruptive behavior, IQ, and later school achievement and delinquent behavior. J. Abnorm. Child Psychol. 23, 183–199.
Haas, H., Panula, P., 2003. The role of histamine and the tuberomamillary nucleus in the nervous system. Nat. Rev. Neurosci. 4, 121–130.
Haber, S.N., 2016. Corticostriatal circuitry. Dialogues Clin. Neurosci. 18, 7–21.
Heal, D.J., Smith, S.L., Kulkarni, R.S., Rowley, H.L., 2008. New perspectives from microdialysis studies in freely-moving, spontaneously hypertensive rats on the pharmacology of drugs for the treatment of ADHD. Pharmacol. Biochem. Behav. 90, 184–197.
Hinshaw, S.P., 1992. Academic underachievement, attention deficits, and aggression: comorbidity and implications for intervention. J. Consult. Clin. Psychol. 60, 893–903.
Jarome, T.J., Kwapis, J.L., Ruenzel, W.L., Helmstetter, F.J., 2013. CaMKII, but not protein kinase A, regulates Rpt6 phosphorylation and proteasome activity during the formation of long-term memories. Front. Behav. Neurosci. 7, 115.
Knouse, L.E., Teller, J., Brooks, M.A., 2017. Meta-analysis of cognitive-behavioral treatments for adult ADHD. J. Consult. Clin. Psychol. 85, 737–750.
Koda, K., Ago, Y., Cong, Y., Kita, Y., Takuma, K., Matsuda, T., 2010. Effects of acute and chronic administration of atomoxetine and methylphenidate on extracellular levels of noradrenaline, dopamine and serotonin in the prefrontal cortex and striatum of mice. J. Neurochem. 114, 259–270.
Leaver, A.M., Renier, L., Chevillet, M.A., Morgan, S., Kim, H.J., Rauschecker, J.P., 2011. Dysregulation of limbic and auditory networks in tinnitus. Neuron 69, 33–43.
Leroy, F., Brann, D.H., Meira, T., Siegelbaum, S.A., 2017. Input-timing-Dependent plasticity in the hippocampal CA2 region and its potential role in social memory. Neuron 95, 1089–1102 e1085.
Lisman, J., Yasuda, R., Raghavachari, S., 2012. Mechanisms of CaMKII action in long-term potentiation. Nat. Rev. Neurosci. 13, 169–182.
Liu, X., Jones, E.G., 1996. Localization of alpha type II calcium calmodulin-dependent protein kinase at glutamatergic but not gamma-aminobutyric acid (GABAergic) synapses in thalamus and cerebral cortex. Proc. Natl. Acad. Sci. 93, 7332.
Liu, X., Jones, E.G., 1997. Alpha isoform of calcium-calmodulin dependent protein kinase II (CAM II kinase-alpha) restricted to excitatory synapses in the CA1 region of rat hippocampus. Neuroreport 8, 1475–1479.
McKay, K.E., Halperin, J.M., 2001. ADHD, aggression, and antisocial behavior across the lifespan. Interactions with neurochemical and cognitive function. Ann. N. Y. Acad. Sci. 931, 84–96.
Messineo, L., Taranto-Montemurro, L., Sands, S.A., Oliveira Marques, M.D., Azabarzin, A., Wellman, D.A., 2017. Broadband sound administration improves sleep onset latency in healthy subjects in a model of transient insomnia. Front. Neurol. 8, 718.
Miller, E.K., Cohen, J.D., 2001. An integrative theory of prefrontal cortex function. Annu. Rev. Neurosci. 24, 167–202.
Molina, B.S., Hinshaw, S.P., Swanson, J.M., Arnold, L.E., Vitiello, B., Jensen, P.S., Epstein, J.N., Hoza, B., Hechtman, L., Abikoff, H.B., Elliott, G.R., Greenhill, L.L., Newcorn, J.H., Wells, K.C., Wigal, T., Gibbons, R.D., Hur, K., Houck, P.R., Group MTAC, 2009. The MTA at 8 years: prospective follow-up of children treated for combined-type ADHD in a multisite study. J. Am. Acad. Child Adolesc. Psychiatry 48, 484–500.
Moss, F., Ward, L.M., Sannita, W.G., 2004. Stochastic resonance and sensory information processing: a tutorial and review of application. Clin. Neurophysiol. 115, 267–281.
Neerad, P., Sumit, M., Ashish, S., Madhuri, J., 2011. Adaptive local thresholding for detection of nuclei in diversity stained cytology images. 2011 International Conference on Communications and Signal Processing. pp. 218–220.
Nestler, E.J., Barrot, M., Self, D.W., 2001. DeltaFosB: a sustained molecular switch for addiction. Proc. Natl. Acad. Sci. U. S. A. 98, 11042–11046.
Nomaru, H., Sakumi, K., Katogi, A., Ohnishi, Y.N., Kajitani, K., Tsuchimoto, D., Nestler, E.J., Nakabeppu, Y., 2014. Fosb gene products contribute to excitotoxic microglial activation by regulating the expression of complement C5a receptors in microglia. Glia 62, 1284–1298.
Ouimet, C.C., McGuinness, T.L., Greengard, P., 1984. Immunocytochemical localization of calcium/calmodulin-dependent protein kinase II in rat brain. Proc. Natl. Acad. Sci. U. S. A. 81, 5604–5608.
Papa, M., Sagvolden, T., Sergeant, J.A., Sadile, A.G., 1996. Reduced CaMKII-positive neurones in the accumbens shell of an animal model of attention-deficit hyperactivity disorder. Neuroreport 7, 3017–3020.
Papa, M., Sergeant, J.A., Sadile, A.G., 1997. Differential expression of transcription factors in the accumbens of an animal model of ADHD. Neuroreport 8, 1607–1612.
Papa, M., Sergeant, J.A., Sadile, A.G., 1998. Reduced transduction mechanisms in the anterior accumbal interface of an animal model of Attention-Deficit Hyperactivity Disorder. Behav. Brain Res. 94, 187–195.
Paxinos, G., Watson, C., 2009. The Rat Brain in Stereotaxic Coordinates, 6th edition. Elsevier, Amsterdam; Boston.
Perrotti, L.I., Hadeishi, Y., Ulery, P.G., Barrot, M., Monteggia, L., Duman, R.S., Nestler, E.J., 2004. Induction of deltaFosB in reward-related brain structures after chronic stress. J. Neurosci. 24, 10594–10602.
Roy, D.S., Kitamura, T., Okuyama, T., Ogawa, S.K., Sun, C., Obata, Y., Yoshiki, A., Tonegawa, S., 2017. Distinct neural circuits for the formation and retrieval of episodic memories. Cell 170, 1000–1012 e1019.
Russell, V.A., 2000. The nucleus accumbens motor-limbic interface of the spontaneously hypertensive rat as studied in vitro by the superfusion slice technique. Neurosci. Biobehav. Rev. 24, 133–136.
Russell, V.A., 2002. Hypodopaminergic and hypernoradrenergic activity in prefrontal cortex slices of an animal model for attention-deficit hyperactivity disorder–the spontaneously hypertensive rat. Behav. Brain Res. 130, 191–196.
Russell, V.A., 2003. Dopamine hypofunction possibly results from a defect in glutamate-stimulated release of dopamine in the nucleus accumbens shell of a rat model for attention deficit hyperactivity disorder–the spontaneously hypertensive rat. Neurosci. Biobehav. Rev. 27, 671–682.
Sadile, A.G., 2000. Multiple evidence of a segmental defect in the anterior forebrain of an animal model of hyperactivity and attention deficit. Neurosci. Biobehav. Rev. 24, 161–169.
Sagvolden, T., 2000. Behavioral validation of the spontaneously hypertensive rat (SHR) as an animal model of attention-deficit/hyperactivity disorder (AD/HD). Neurosci. Biobehav. Rev. 24, 31–39.
Santosh, P.J., Sattar, S., Canagaratnam, M., 2011. Efficacy and tolerability of pharmacotherapies for attention-deficit hyperactivity disorder in adults. CNS Drugs 25, 737–763.
Sanz-Blasco, S., Bordone, M.P., Damianich, A., Gomez, G., Bernardi, M.A., Isaja, L., Taravini, I.R., Hanger, D.P., Avale, M.E., Gershanik, O.S., Ferrario, J.E., 2018. The kinase fyn As a novel intermediate in L-DOPA-induced dyskinesia in Parkinson's disease. Mol. Neurobiol. 55, 5125–5136.
Satterfield, J., Swanson, J., Schell, A., Lee, F., 1994. Prediction of antisocial behavior in attention-deficit hyperactivity disorder boys from aggression/defiance scores. J. Am. Acad. Child Adolesc. Psychiatry 33, 185–190.
Schindelin, J., Arganda-Carreras, I., Frise, E., Kaynig, V., Longair, M., Pietzsch, T., Preibisch, S., Rueden, C., Saalfeld, S., Schmid, B., Tinevez, J.Y., White, D.J., Hartenstein, V., Eliceiri, K., Tomancak, P., Cardona, A., 2012. Fiji: an open-source platform for biological-image analysis. Nat. Methods 9, 676–682.
Shier, A.C., Reichenbacher, T., Ghuman, H.S., Ghuman, J.K., 2013. Pharmacological treatment of attention deficit hyperactivity disorder in children and adolescents: clinical strategies. J. Cent. Nerv. Syst. Dis. 5, 1–17.
Sikström, S., Söderlund, G., 2007. Stimulus-dependent dopamine release in attention-deficit/hyperactivity disorder. Psychol. Rev. 114, 1047–1075.
Söderlund, G., Sikström, S., Smart, A., 2007. Listen to the noise: noise is beneficial for cognitive performance in ADHD. J. Child Psychol. Psychiatry 48, 840–847.
Söderlund, G.B., Sikström, S., Loftesnes, J.M., Sonuga-Barke, E.J., 2010. The effects of background white noise on memory performance in inattentive school children. Behav. Brain Funct. 6, 55.
Söderlund, G.B., Eckernäs, D., Holmblad, O., Bergquist, F., 2015. Acoustic noise improves motor learning in spontaneously hypertensive rats, a rat model of attention deficit hyperactivity disorder. Behav. Brain Res. 280, 84–91.
Söderlund, G.B., Bjork, C., Gustafsson, P., 2016. Comparing auditory noise treatment with stimulant medication on cognitive task performance in children with attention deficit hyperactivity disorder: results from a pilot study. Front. Psychol. 7, 1331.
Spencer, T., Biederman, J., Wilens, T., Harding, M., O'Donnell, D., Griffin, S., 1996. Pharmacotherapy of attention-deficit hyperactivity disorder across the life cycle. J. Am. Acad. Child Adolesc. Psychiatry 35, 409–432.
Stanchina, M.L., Abu-Hijleh, M., Chaudhry, B.K., Carlisle, C.C., Millman, R.P., 2005. The influence of white noise on sleep in subjects exposed to ICU noise. Sleep Med. 6, 423–428.
Steinhausen, H.C., Novik, T.S., Baldursson, G., Curatolo, P., Lorenzo, M.J., Rodrigues Pereira, R., Ralston, S.J., Rothenberger, A., Group AS, 2006. Co-existing psychiatric problems in ADHD in the ADORE cohort. Eur. Child Adolesc. Psychiatry 15 (Suppl 1), I25–29.
Swanson, J.M., et al., 2017. Young adult outcomes in the follow-up of the multimodal treatment study of attention-deficit/hyperactivity disorder: symptom persistence, source discrepancy, and height suppression. J. Child Psychol. Psychiatry 58, 663–678.
Tada, H., Miyazaki, T., Takemoto, K., Takase, K., Jitsuki, S., Nakajima, W., Koide, M., Yamamoto, N., Komiya, K., Suyama, K., Sano, A., Taguchi, A., Takahashi, T., 2016. Neonatal isolation augments social dominance by altering actin dynamics in the medial prefrontal cortex. Proc. Natl. Acad. Sci. U. S. A. 113, E7097–E7105.
Thomas, R., Sanders, S., Doust, J., Beller, E., Glasziou, P., 2015. Prevalence of attention-deficit/hyperactivity disorder: a systematic review and meta-analysis. Pediatrics 135, e994–1001.
Torrent, A., Moreno-Delgado, D., Gomez-Ramirez, J., Rodriguez-Agudo, D., Rodriguez-Caso, C., Sanchez-Jimenez, F., Blanco, I., Ortiz, J., 2005. H3 autoreceptors modulate histamine synthesis through calcium/calmodulin- and cAMP-dependent protein kinase pathways. Mol. Pharmacol. 67, 195–203.
Wood, S., Sage, J.R., Shuman, T., Anagnostaras, S.G., 2014. Psychostimulants and cognition: a continuum of behavioral and cognitive activation. Pharmacol. Rev. 66, 193–221.
Yabuki, Y., Shioda, N., Maeda, T., Hiraide, S., Togashi, H., Fukunaga, K., 2014. Aberrant CaMKII activity in the medial prefrontal cortex is associated with cognitive dysfunction in ADHD model rats. Brain Res. 1557, 90–100.
Zentall, S.S., Zentall, T.R., 1983. Optimal stimulation: a model of disordered activity and performance in normal and deviant children. Psychol. Bull. 94, 446–471.
Zhong, W., Hutchinson, T.E., Chebolu, S., Darmani, N.A., 2014. Serotonin 5-HT(3) receptor-mediated vomiting occurs via the activation of Ca(2+)/CaMKII-Dependent ERK1/2 signaling in the least shrew (Cryptotis parva). PLoS One 9, e104718.